RESEARCH ARTICLE

AMERICAN JOURNAL OF BOTANY

INVITED PAPER

For the Special Issue: Evolutionary Insights from Studies of Geographic Variation

Predicting the genetic consequences of future climate change: The power of coupling spatial demography, the coalescent, and historical landscape changes[1]

Jason L. Brown[2,6], Jennifer J. Weber[5], Diego F. Alvarado-Serrano[2], Michael J. Hickerson[2–4], Steven J. Franks[5], and Ana C. Carnaval[2,3]

PREMISE OF THE STUDY: Climate change is a widely accepted threat to biodiversity. Species distribution models (SDMs) are used to forecast whether and how species distributions may track these changes. Yet, SDMs generally fail to account for genetic and demographic processes, limiting population-level inferences. We still do not understand how predicted environmental shifts will impact the spatial distribution of genetic diversity within taxa.

METHODS: We propose a novel method that predicts spatially explicit genetic and demographic landscapes of populations under future climatic conditions. We use carefully parameterized SDMs as estimates of the spatial distribution of suitable habitats and landscape dispersal permeability under present-day, past, and future conditions. We use empirical genetic data and approximate Bayesian computation to estimate unknown demographic parameters. Finally, we employ these parameters to simulate realistic and complex models of responses to future environmental shifts. We contrast parameterized models under current and future landscapes to quantify the expected magnitude of change.

KEY RESULTS: We implement this framework on neutral genetic data available from *Penstemon deustus*. Our results predict that future climate change will result in geographically widespread declines in genetic diversity in this species. The extent of reduction will heavily depend on the continuity of population networks and deme sizes.

CONCLUSIONS: To our knowledge, this is the first study to provide spatially explicit predictions of within-species genetic diversity using climatic, demographic, and genetic data. Our approach accounts for climatic, geographic, and biological complexity. This framework is promising for understanding evolutionary consequences of climate change, and guiding conservation planning.

KEY WORDS climate change; conservation; demographic inference; *Penstemon deustus*; Plantaginaceae; spatial coalescent; species distribution models

Predicting how intraspecific genetic diversity is influenced by rampant environmental changes triggered by humans is central for conservation and essential for the maintenance of global eco- and evosystem services (Dawson et al., 2011). Numerous studies have emphasized the association between evolutionary potential and genetic diversity, as diversity provides the raw material for evolution (e.g., Barrett and Schluter, 2008; Prentis et al., 2008; Jump et al., 2009; Takahashi and Katano, 2010; Alsos et al., 2012). Genetic diversity has been shown to play a key role in both the past and future trajectory of species, with mounting evidence in studies of climate change (e.g., Garner et al., 2005; Alsos et al., 2009, 2012; Taubmann et al., 2011). Because only a portion of standing genetic variation will be adaptive under given environmental conditions, genotypes of quantitative traits are often seen as ideal targets for understanding evolutionary potential (Reed and Frankham, 2001). However, data on quantitative traits are frequently unavailable, and it is often difficult to predict which traits will be most relevant under changing environments. Opportunely, correlations do exist between differentiation of quantitative traits and neutral markers (Frankham et al., 1999; Merila and Crnokrak, 2001; Leinonen et al., 2008; Jump et al., 2009). In fact, with the unpredictable nature of climate change and the difficulty of determining which traits would be most relevant in changing environments, genetic diversity measures from widely available neutral markers may be one of our best estimates of adaptive potential in naturally occurring populations (Humphries et al., 1995; Jump et al., 2009).

[1] Manuscript received 21 March 2015; revision accepted 14 July 2015.

[2] Biology Department, The City College of New York, New York, New York 10031 USA;
[3] The Graduate Center, City University of New York, New York, New York 10016 USA;
[4] Department of Invertebrate Zoology, American Museum of Natural History, New York, New York 10024 USA; and
[5] Department of Biological Sciences, Fordham University, Bronx, New York 10458 USA
[6] Author for correspondence (e-mail: jasonleebrown@gmail.com)

doi:10.3732/ajb.1500117

Recent studies have explored the use of spatial interpolation (Espíndola et al., 2012), generalized dissimilarity modeling (Fitzpatrick and Keller, 2015), or categorization (Alsos et al., 2012; Yannic et al., 2014) of contemporary genetic landscapes to estimate changes in the genetic diversity of populations under future climates. While these methods constitute a substantial step forward for predicting the future genetic composition of species, they do not account for spatially explicit changes in population densities, explicit population histories, or migration rates due to habitat changes. Here, we address these issues while moving beyond predictions of species presences or absences in the future. Our goal is to implement a novel framework to predict the impact of future climate shifts on the spatial distribution of neutral genetic diversity within species.

To shed new light into the potential evolutionary consequences of anthropogenic environmental change (Parmesan and Yohe, 2003), we expand on the use of species distribution models (SDMs). This tool has been widely used to predict how the range of populations will shift in response to climate change (reviewed by Alvarado-Serrano and Knowles, 2014; Fordham et al., 2014). SDMs estimate habitat suitability across a landscape and are typically created by inferring the ecological tolerances of a species from observed locality data (Peterson et al., 2011). Once a model is trained with available occurrence records, it can be projected onto a geographical area at current, past, or future times. To date, hundreds of studies have used correlative SDMs (e.g., Maxent or Random Forests; Peterson et al., 2011) to quantify changes in habitat suitability over time (e.g., Graham et al., 2010; Anderson, 2013; Assis et al., 2014). Yet, these methods have garnered criticism when used for prediction of species' responses to environmental change given the somewhat simplistic assumptions used for model projection. For instance, SDMs often fail to account for dispersal abilities or barriers. In many cases, it remains uncertain whether habitats predicted as suitable under future climatic conditions can actually be colonized (Peterson et al., 2011; Anderson, 2013).

Genetic data, when merged with spatial analyses, can provide a key missing part of this equation (Chan et al., 2011; Marske et al., 2012). Recent approaches have been building upon the use of SDMs by coupling them with coalescent analyses that allow for a better understanding of how demographic processes impact (or impacted) populations, both now and in the past (Knowles and Alvarado-Serrano, 2010; Brown and Knowles, 2012; Gehara et al., 2013; He et al., 2013; Dellicour et al., 2014). Specifically, these studies have employed SDMs to infer temporally specific landscape suitability and landscape dispersal permeability, which represents the ease of dispersal from one locality to another. Using this information, mechanistic demographic models based on empirical life-history data (generation times and growth rates) have been built to assess how the distribution of a species, and local density, changed from the past to the present. Based on this estimated colonization history, coalescent genealogies can be simulated from current time into the past, characterizing the entire genetic landscape (Knowles and Alvarado-Serrano, 2010; Brown and Knowles, 2012; Gehara et al., 2013; He et al., 2013).

We further expand on these spatial coalescent-based analyses and build on inferences about past population responses to environmental change to predict key demographic and genetic parameters of populations, particularly aimed at flagging potential changes in population sizes and genetic diversity under future environmental conditions. This paper is a demonstration of our method and, before any genetic measurements can be used with confidence to guide conservation efforts, evaluation of additional demographic scenarios and measurements of model uncertainty need to quantified (see Discussion for information on these improvements). To implement this framework, we used locality and genetic data from the widely distributed herbaceous species *Penstemon deustus* (Plantaginaceae). We carefully parameterized SDMs under present environmental conditions and projected these models into past and future climates in western North America to obtain temporally dynamic estimates of the spatial distribution of suitable habitats and landscape dispersal permeability for this species. Because accurate estimates of several key demographic parameters that are essential for the assessment of species-specific responses to climate change are unknown for most species, including *P. deustus*, we use empirical genetic data (intraspecific DNA sequences) analyzed under an approximate Bayesian computation (ABC) framework to glance into the past and to estimate these key demographic parameters (i.e.; long-term migration rates, maximum landscape carrying capacity, and ancestral population sizes) for our target species. We then employed these parameter estimates to predict into the future by building demographic and spatial genetic models of future landscapes and quantifying the expected impact of climate change on the spatial distribution of genetic variation within *P. deustus* (see Fig. 1 for graphic overview). By using the spatial coalescent as a lens to understand historical population demography, we make better-informed and more realistic predictions about the potential genetic outcomes of ongoing and future changes.

MATERIALS AND METHODS

Study species—We focused this study on *Penstemon deustus* (Plantaginaceae) Douglas ex Lindl. var. *pedicellatus* M.E.Jones, a widespread and common herbaceous species in northwestern North America (Kartesz, 1999; Fig. 2A, C). The species occurs in sagebrush habitat and on rocky slopes on sky islands (ca. >1000 m a.s.l.) in the Cascade Range and Great Basin. *Penstemon deustus* is a perennial with many small flowers, blooming early in the spring. Flowers are protandrous and exhibit some self-compatibility with mixed mating systems (Kramer, 2008). Seed dispersal is generally by gravity, though seeds may occasionally be carried by wind along the ground (Fuller and del Moral, 2003). Pollination is primarily by small bees and some bumblebees (several *Osmia* spp. and *Bombus* spp.; Kramer et al., 2011). Local population sizes and densities range from 100 to 500 or more flowering plants (Kramer et al., 2011).

Population genetic data of *P. deustus* were obtained from Kramer et al. (2011), with permission from the authors. Kramer et al. (2011) sampled eight localities across four mountain ranges of the Great Basin region (two localities per mountain range). More than 100 plants were sampled per locality. Using a set of seven microsatellite markers, Kramer et al. (2011) showed that *P. deustus* has significant genetic structure (F_{ST} = 0.133, R_{ST} = 0.407). This strong genetic subdivision suggested limited admixture between populations both within and among mountain ranges. Mantel tests revealed significant isolation by geographic distance with both F_{ST} and R_{ST} (Mantel test, F_{ST} P = 0.02; R_{ST} P = 0.01). Further analyses suggested limited gene flow north–south and east–west. Population-level inbreeding was significant in four of the eight sampled populations.

***Occurrence data*—**We compiled 984 occurrence localities of *P. duestus* from primary literature and the Global Biodiversity Information Facility (www.GBIF.org). All occurrence localities were vetted for spatial and taxonomic accuracy. Points that met one or more of the following criteria were removed: (1) taxonomic uncertainty, (2) low coordinate precision, (3) coordinates grossly outside of the known range (as reported by Kartesz, 2015), or (4) coordinates that precisely matched counties' centroids (indicating general range information rather than specific population location). Spatial sampling biases in the filtered occurrence data were corrected with SDMToolbox, a python-based ArcGIS toolbox (Brown, 2014), by rarefying the localities and randomly selecting a single occurrence point when many were present within a shared area at a 10 km^2 spatial resolution. We used a 10 km^2 radius to rarefy the localities because it retained spatially independent data in regions of high habitat and topographic heterogeneity, while considerably reducing spatial autocorrelation between occurrence localities and the climate data used here (as measured in the program SAM v4.0 using a spatial correlogram, Rangel et al., 2010). The resulting 361 localities were used for modeling (Appendix S1, see Supplemental Data with the online version of this article).

Climate data—Climate data under present-day conditions were composed of a subset of the original standard Bioclim variables (n = 8; Bio1, 4, 10–12, 15–17) at 2.5 arc-minute resolution, downloaded from the Worldclim Global Climate Data website (www.worldclim.org; Hijmans et al., 2005). This subset corresponds to bio-climate variables that are also available for past periods. Past climate data were taken from snapshot climatic simulations spanning the last 50 kyr using the Hadley Centre Climate model (HadCM3, Singarayer and Valdes, 2010; Fuchs et al., 2013), from which climatic reconstructions are available at short (1–4 kyr) time intervals. The fine-interval climate data enable a more continuous and dynamic view of habitat suitability through time. Climatic data for four future climate time periods (2030, 2050, 2070, and 2080) were obtained from the most recent Hadley Centre Climate model (HadGEN2-ES) provided by the 5th IPCC climate assessment (IPCC, 2014). We used the RCP 6.0 emission scenario to represent moderate temperature change. This model projects a future world of rapid economic growth, new and more efficient energy technologies, and convergence between regions (IPCC, 2014). The RCP 6.0 scenario is most similar to the former IPCC v4 A1B scenario and adopts a balance across all energy sources (fossil and renewable) for the technological change in the energy system (IPCC, 2014). This and the A1B scenarios have been extensively used to represent a medium emission trajectory (van der Linden and Mitchell, 2009), resulting in mid-range estimates of average global changes (IPCC, 2014). We did not include alternative scenarios because our focus was on assessing the relative power of our approach in comparison to traditional uses of SDMs. For an accurate estimation of spatial predictions of the genetic consequences of future climate change, additional emission scenarios and climate models need to be evaluated.

Species distribution models—Species distribution models (SDMs) for *P. deustus* were generated in the program MaxEnt v3.3.3k (Phillips et al., 2006). Models were built on the entire range of the species (western North America, as depicted in Fig. 2Cii) and later clipped to the extent of this study (Fig. 2Ci; 43.736N, −120.972W by 35.236N, −112.129W). To reduce issues associated with background selection and unoccupied, climatically suitable habitat (see Anderson and Raza, 2010; Barbet-Massin et al., 2012; Merow et al., 2013), a minimum convex polygon was created from occurrence localities to which a 100 km buffer was applied. This area was used for background point selection for modeling (performed in SDMtoolbox v1.1b). To properly parameterize models, we (1) performed a spatial jackknifing of the background and occurrence points, and (2) independently evaluated all model feature classes (the type of mathematic relationship assessed between the environmental data and occurrence data) and several regularization multiplier factors (which condition how closely the model fits the occurrence points, with greater values allowing a more spread out distribution; see Peterson et al., 2011; Shcheglovitova and Anderson, 2013; Alvarado-Serrano and Knowles, 2014; Boria et al., 2014; Radosavljevic and Anderson, 2014). Given our sample size of 341 localities, we evaluated the performance of five combinations of feature classes [linear (1), linear and quadratic (2), hinge (3), linear, quadratic and hinge (4) and linear, quadratic, hinge, product and threshold (5)], and for every regularization multiplier value tested (which ranged between 0.5 and 5 in increments of 0.5; see Phillips and Dudik, 2008; Shcheglovitova and Anderson, 2013; Radosavljevic and Anderson, 2014; Brown, 2014 for details).

Models were evaluated by geographically structured k-fold cross-validation, a method that tests evaluation performance of spatially segregated localities (k = 5, SDMtoolbox 1.1b; Brown, 2014). Model fit was evaluated by omission rate, area under the curve (AUC), and model feature class complexity, in the order listed (see Brown, 2014 for details). After the optimum model parameters were determined (those showing a model with the lowest omission rate, highest AUC, and lowest complexity), a final model was built using all localities together. This model was then projected to all future and past climates. When predicting for variable values outside the range found in the study area, all projections of the response curves of the final model were reset ("clamped") to match the upper or lower values found in the study area (Phillips et al., 2006).

***Transforming SDMs into demographic parameters*—**The SDMs were rendered into two components for use in the demographic simulations: (1) friction landscapes (F_l) and (2) carrying capacity landscapes (K_l; see Knowles and Alvarado-Serrano, 2010; Brown and Knowles, 2012 for a detailed overview of methods). In brief, the SDM values were rescaled for friction landscapes so that values ranged from zero to one and then inverted. The resulting F_l, defining the relative difficulty of movement of individuals between demes, depicted areas of high predicted habitat suitability as having low friction values to dispersal. In our demographic models, the number of emigrants per generation was the result of the migration rate (m, the per generation probability that an individual moves out of a deme) and the total number of occupants in that deme (which in turn depended on the local carrying capacity, k, and the logistic growth parameter, r). The spatial distribution of emigrants in each generation is associated with the friction values of neighboring demes. Friction and carrying capacity landscapes were created for the 41 time periods with climate data available. Before ABC analyses, we tested six common demographic transformations (transformation type: linear, sigmoid, binary; and two μ values for each transformation type; Brown and Knowles, 2012). Here we used a single scenario, a sigmoid conversion, to convert the SDM into K_l and F_l (with F_l being the inverse of K_l; see Brown and Knowles, 2012

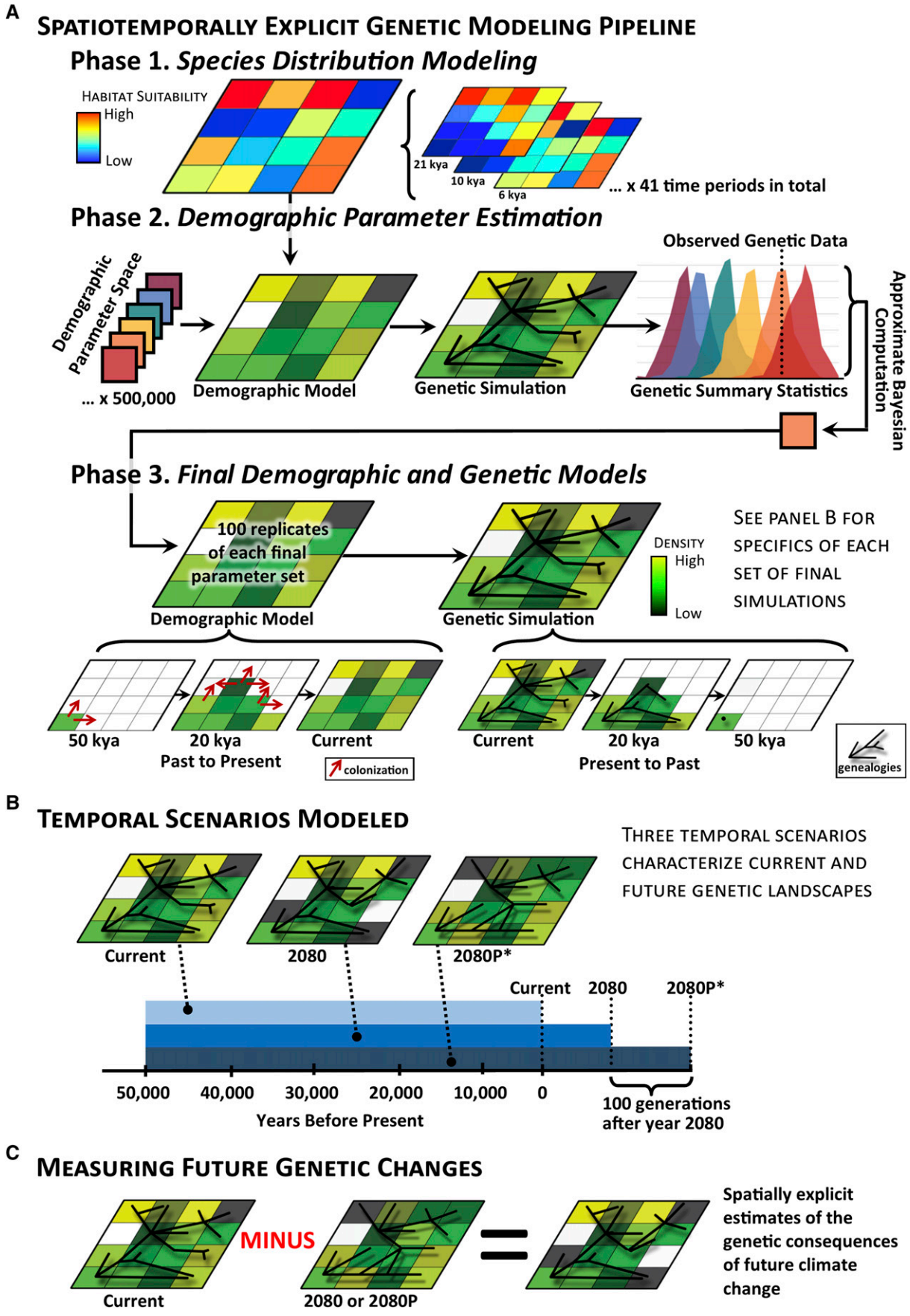
A
SPATIOTEMPORALLY EXPLICIT GENETIC MODELING PIPELINE
Phase 1. Species Distribution Modeling
HABITAT SUITABILITY
High
Low
21 kya
10 kya
6 kya
... x 41 time periods in total
Phase 2. Demographic Parameter Estimation
Demographic Parameter Space
... x 500,000
Demographic Model
Genetic Simulation
Observed Genetic Data
Genetic Summary Statistics
Approximate Bayesian Computation
Phase 3. Final Demographic and Genetic Models
100 replicates of each final parameter set
Demographic Model
Genetic Simulation
DENSITY
High
Low
SEE PANEL B FOR SPECIFICS OF EACH SET OF FINAL SIMULATIONS
50 kya
20 kya
Past to Present
Current
colonization
Current
20 kya
Present to Past
50 kya
genealogies
B
TEMPORAL SCENARIOS MODELED
THREE TEMPORAL SCENARIOS CHARACTERIZE CURRENT AND FUTURE GENETIC LANDSCAPES
Current
2080
2080P*
Current
2080
2080P*
50,000
40,000
30,000
20,000
10,000
0
Years Before Present
100 generations after year 2080
C
MEASURING FUTURE GENETIC CHANGES
MINUS
Current
2080 or 2080P
Spatially explicit estimates of the genetic consequences of future climate change

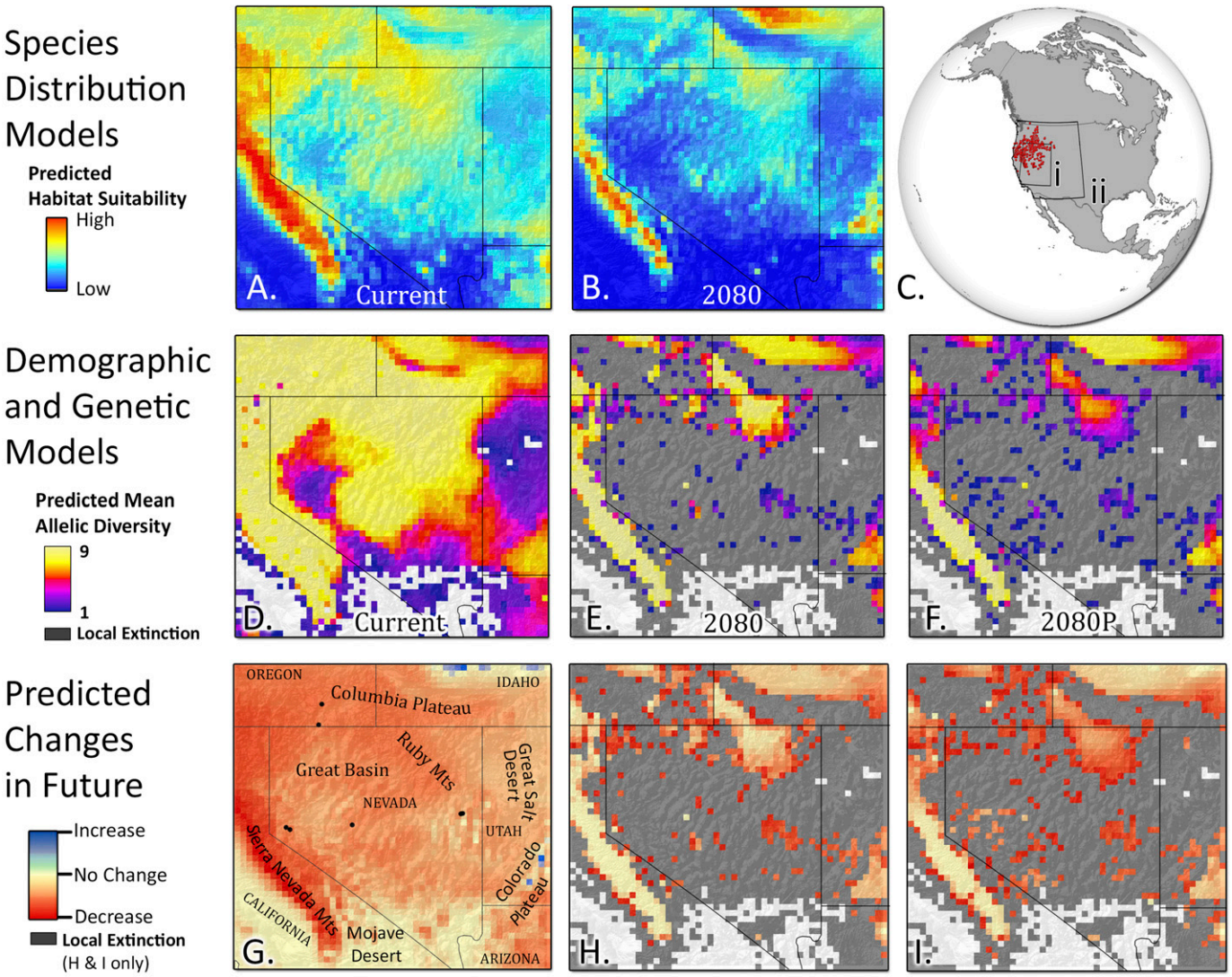

FIGURE 2 Predicted habitat suitability and genetic changes due to future climate change. Species distribution models for (A) current time periods and (B) 2080. (Ci) Overview of demographic modeling extent and (Cii) SDM modeling extent along with vetted localities. Results from demographic and genetic modeling for the three time periods: (D) current, (E) 2080, (F) 2080 plus 100 generations. Future change landscapes: (G) Predicted changes in habitat suitability by 2080 as predicted from SDMs. Dots in this plot depict the localities with empirical genetic data that were used for ABC parameter estimation. (H) Modeled genetic changes by 2080 and by (I) 2080 plus 100 generations.

for details) because it best matched current distribution data and population densities. The final transformation was done by using a normal cumulative distribution function, where the inflection point of the sigmoidal curve, μ, was 0.510 and the slope of the curve, σ, was 0.084. These values were obtained from corresponding current SDM values measured at observed localities, where the lower quartile equaled μ and half of the standard deviation equaled σ (see Brown and Knowles, 2012 for a detailed explanation and discussion of these parameters). The ABC analyses required extensive computational time and our ability to evaluate alternative transformation scenarios was limited. For an accurate estimation of spatial predictions of the genetic consequences of future climate change, additional demographic transformation scenarios must be evaluated in ABC analyses (see Brown and Knowles, 2012 for an overview of this).

←

FIGURE 1 Overview of spatiotemporally explicit modeling of genetic changes due to future climate change. (A) An overview of the modeling pipeline. Three phases occur: species distribution modeling at different time periods characterized the spatiotemporal distribution of suitable habitats and dispersal potential through the landscape. Unknown demographic parameters (here migration rate, deme maximum carrying capacity, and effective ancestral population size) are estimated using approximate Bayesian computation (ABC) by comparing how well simulations based on a wide range of biologically relevant values emulate the observed genetic values. Lastly, ABC-estimated demographic parameters are run in final simulations for various time periods. Genetic simulations are run backward in time using the simulated colonization history from forward time demographic models. (B) Three temporal scenarios modeled in this paper in the third step of our pipeline. (C) Spatially explicit measurements of future genetic change.

***Demographic and spatial genetic modeling*—**A two-dimensional-stepping stone, forward-in-time demographic colonization process (Kimura and Weiss, 1964) was simulated based on the per-deme maximum carrying capacity, migration, and density limitations imposed by the SDMs (i.e., by the F_l and K_l landscapes), using the program SPLATCHE 2 (Ray et al., 2010). During demographic modeling, the colonization of the landscape proceeded in a generation-by-generation manner initiated from of individuals in a predetermined ancestral source area(s). During each generation, population growth in each deme followed a logistic model characterized by a per-generation intrinsic rate (r) and the time-specific SDM-informed maximum carrying capacity (K_l). This step was immediately followed by migration of individuals into neighboring demes conditioned by the time-specific SDM-based friction of the landscape (F_l). A spatial resolution of 20 km^2 was used for the demographic modeling because the spatial autocorrelation of the observed genetic data approached zero at this resolution (measured in SAM v4.0 using a spatial correlogram; Rangel et al., 2010).

A total of 500,000 forward-in-time simulations, in which the colonization of contemporary populations were dependent upon the demographic and environmental parameters, were performed under different parameter settings (see below). Each one of these simulations was then followed by a corresponding backward-in-time coalescent simulation parameterized by the spatially explicit demographic conditions simulated first. Specifically, the record of the per-generation movement of individuals and deme population sizes from the demographic simulations informed the probability of within deme coalescent events and the probability of each sampled gene backward-in-time movement to neighboring demes. Genes from focal populations were sampled from the resulting genealogies (see Excoffier et al., 2000; Currat et al., 2004; Knowles and Alvarado-Serrano, 2010; Ray et al., 2010; and Brown and Knowles, 2012 for an overview of data flow and input parameters).

A logistic growth rate of 0.2 and a generation time of 10 yr were fixed in all demographic simulations. This long generation time had to be employed due to computational limitations on the number of generations and spatial resolution. To adjust the simulations to the actual generation time, which is ca. 1 yr (Kramer et al., 2011), we multiplied the observed mutation, recombination and growth rates by 10 in all simulations. This ensured that the modeled rates match the true history of the species and the tempo of climate change represented in our SDMs.

Initial population densities and the spatial location of historic occurrences used to initialize demographic models were obtained from the top 1/10 quantile of SDM values observed in the 50 kya SDM (Knowles and Alvarado-Serrano, 2010). The maximum number of individuals allowed in each simulation (i.e., the maximum per deme carrying capacity) was allotted to each "presence" cell at the start of the simulations. If the cell's actual carrying capacity, as informed by the corresponding projected SDM, was lower than the maximum capacity (i.e., if their suitability was lower than the maximum), the remaining individuals were distributed in neighbor cells.

For the genetic simulations, we focused on conditions that matched the empirical microsatellite data set of Kramer et al. (2011). Specifically, all simulated genetic data matched the empirical data in the number of loci sequenced (seven), the number of base pairs per locus, the corresponding models of nucleotide substitution, and the number of individuals per sampling locality (eight populations with 32 individuals each; Table 1). Specifically, the following seven dinucleotide microsatellite loci were simulated using specific dinucleotide repeat motif mutation rates as measured from the genome of *Arabidopsis thaliana* (Marriage et al., 2009): *Loc2* (1.96×10^{-4} mutations per allele per generation), *Loc4* (3.31×10^{-4}), *Loc5* (3.31×10^{-4}), *Loc6* (2.1×10^{-4}), *Loc18* (1.9×10^{-4}), *Loc23* (3.31×10^{-4}), *Loc24* (2.49×10^{-4}). Rates of recombination were set to 4.80 cM/Mb based on genomic averages in *Arabidopsis* and rice (Rizzon et al., 2006).

***Demographic parameter estimation*—**Real populations often lack accurate estimates of key demographic parameters such as long-term migration rates, maximum landscape carrying capacity, and ancestral population sizes, which are essential for the assessment of species-specific responses to climate change. The lack of these key parameters represents a challenge when generating realistic scenarios of the future genetic constitution of species and populations. In the novel approach we propose here, the historical values of these critical demographic parameters are estimated using approximate Bayesian computation (ABC) (Beaumont et al., 2002; Bertorelle et al., 2010; Csilléry et al., 2010). In this statistical approach, parameter estimates are obtained by using statistics to summarize the data and simulations. Basically, under the ABC, paradigm simulations are performed following a hypothesized model (in our case informed by the set of time-specific SDMs and the known biology of *P. deustus*), under an array of parameter values chosen from a bounded probability distribution (Table 2). Each simulation, as well as the observed data (set of microsatellite sequences in our case), is condensed into a set of summary statistics, and the set of simulations that most closely resemble the observed data is then used to estimate the most likely parameters' value and uncertainty (Csilléry et al., 2010).

Following the ABC framework outlined by He et al. (2013), we used ABCsampler from the ABCtoolbox v1.0 package (Wegmann et al., 2010) to perform 500,000 coupled demographic-coalescent simulations under a wide range of parameter values (Table 2). These simulations were consistent with those of Kramer et al., 2011 and other research on *P. deustus* (Kartesz, 1999; Kramer, 2008; Kartesz, 2015). We removed all simulations in which any of the sampling localities (Fig. 2G) had fewer individuals than the empirically sample at any given locality. The remaining 448,967 simulations were summarized into a total of 140 commonly used summary statistics (Table 2) that were calculated from the simulated (as well as empirical) microsatellite sequences using a command line version of the program Arlequin v3.5 (Excoffier and Lischer, 2010). This set of 140 summary statistics provided an ample characterization of inter- and intra-population genetic variation (Appendix S2, see the online Supplemental Data); Wegmann et al., 2009; Beaumont et al., 2010; Excoffier and Lischer, 2010) and were all informative for model parameter estimation as demonstrated by the moderate to strong correlation with the free model parameters (online Appendix S3). Yet, because many of these statistics were highly correlated with each other, and given that ABC estimation accuracy is often reduced due to the impossibility of finding simulated data sets close to the empirical data when dimensionality is high (Beaumont et al., 2010; Blum, 2010), following Wegmann et al. (2009), we transformed this large set of statistics into partial least squares (PLS) components (Wold, 1966; Boulesteix and Strimmer, 2007). These PLS components, which are orthogonal linear combinations of summary statistics that maximize the covariance between statistics

TABLE 1. Empirical population and genetic information on observed populations: spatial data, population size and microsatellites summary statistics for focal populations used in this study (all data from Kramer et al., 2011).

Focal population information						Empirical genetic data			
Locality	State	Latitude	Longitude	Elevation (m)	Population size	*N* independently sampled	Mean alleles per locus	Private alleles	Observed H_e
Desatoya Mountains	NV	39.25	−117.68	2025	100–150	32	14.7	8	0.736
Desatoya Mountains	NV	39.24	−117.78	1909	400 –500	32	10.7	4	0.736
Schell Creek Range	NV	39.56	−114.64	2649	200–300	32	7.9	1	0.674
Schell Creek Range	NV	39.57	−114.5	2022	200–300	32	9.6	5	0.693
Steens Mountains	OR	42.63	−118.53	1793	200–300	32	14.7	23	0.744
Steens Mountains	OR	42.05	−118.62	1368	200–300	32	11.0	8	0.74
Pine Nut Mountains	NV	39.18	−119.53	1861	150–200	32	12.4	1	0.758
Pine Nut Mountains	NV	39.12	−119.42	1834	150–200	32	11.3	3	0.723

and parameters, were computed using the first 10,000 simulations as random calibration. After exploring the reduction of the root mean-squared errors associated with each additional PLS component for each parameter (online Appendices S3, S4); for details, see Wegmann et al., 2009), we retained only the first 10 PLS components.

The ABC estimation was performed using ABCestimator from the ABCtoolbox v1.0 package (Wegmann et al., 2010), under a standard ABC rejection approach (Tavaré et al., 1997; Beaumont et al., 2002). Summary statistics from each simulation were first transformed into the PLS components previously computed, using transformer from the ABCtoolbox v1.0 package (Wegmann et al., 2010). The 2250 retained simulations (0.5%) closest to the empirical genetic data were retained. Posterior distributions of the parameters were then calculated based on this closest data set, after performing post-sampling regression adjustment by the ABC-general linear model approach (Leuenberger and Wegmann, 2010). We verified the fit of the model to the empirical data by assessing the fraction of retained simulations that have a smaller or equal likelihood than the observed data, with a small fraction suggesting that the model does not fit well the empirical data (Wegmann et al., 2010). In addition, we assessed the accuracy of the parameter estimation by calculating the coefficient of determination (R^2) between each parameter and the 10 retained PLS components (Neuenschwander et al., 2008).

Estimating the genetic consequences of future climate change— To estimate the genetic consequences of future climate change, three sets of simulations were run. All demographic simulations started 50 kya, but ended at different periods: a current period (ca. year 2010) and two future scenarios (year 2080 and year 2080 plus 100 generations, the latter scenario referred hereafter as 2080p). The 2080p scenario was included because genetic processes are known to lag behind demographic processes; thus, populations were simulated using the 2080 climate for an additional 100 generations. For each time scenario, the mode of the posterior probability of ancestral population size, of the migration rate, and of carrying capacity parameters (all inferred by ABC as previously stated) were used. All other parameters, including growth rate, were kept at the same values used for the simulations above. Genetic constitution of every occupied locality at the end of the demographic model was sampled (on average, 2094 grid cells for current and 559 for 2080/2080p). Demographic and genetic simulations were repeated 100 times for each of the three temporal scenarios, through 20 replicate demographic models, each with five genetic simulation replicates (Gehara et al., 2013). The measured genetic changes for each future scenario were subtracted from the current genetic landscape to measure predicted genetic changes. Because output summary statistics of the simulated genetic data were highly correlated (r^2 = 0.93, $p < 0.001$), we chose to only present mean allelic diversity here, which depicts the average allelic diversity (r) among the seven simulated microsatellites.

RESULTS

Species distribution models—We evaluated 250 different SDMs based on different model parameters (feature class type and regularization multipliers) and input training/test data (k-fold cross-validation). The best performing model was the one parameterized with linear and quadratic feature classes and a regularization multiplier of 2 (Fig. 2A). This model's high predictive accuracy is indicated by an average omission rate of spatially independent test data of 0.205 and an average AUC of spatial independent data of 0.991. Projecting this model using the future climate change scenario, habitat suitability is predicted to dramatically decline throughout the landscape (Fig. 2B, G), with highest declines in suitability values in the Sierra Nevada Mountains, and widespread reductions predicted throughout the Great Basin. Only a few localities are estimated to increase habitat suitability by 2080 (i.e., the Rocky Mountains in Idaho or Colorado Plateau in southern Utah).

Demographic parameter estimates—Taking advantage of coupled demographic and coalescent simulations, our ABC analyses allowed

TABLE 2. Distributions of the posterior probabilities of each estimated demographic parameter: long-term migration rate (m), maximum landscape carrying capacity (maxK, in terms of population size), and an ancestral effective population size (N_{eA}). All values are in $\log_{10}$; note that all parameters are estimated at the spatial resolution of simulations.

Parameter	Prior	R^2	Posterior mode	Posterior HPDI 50	Posterior HPDI 90
$\log_{10}$ maxK	U[3, 5]	0.083	4.713	4.677 to 4.747	4.625 to 4.791
$\log_{10} m$	U[−3, −0.2]	0.198	−1.335	−1.626 to −1.147	−2.992 to −0.943
$\log_{10} N_{eA}$	U[2, 4]	0.309	2.00	2.000 to 2.020	2.00 to 2.070

us to estimate three key demographic parameters. Estimates of both long-term migration rates (m) and maximum landscape carrying capacity (maxK) show relatively narrow confidence intervals within the parameter ranges explored. Ancestral population size was more difficult to estimate, as depicted by its right-skewed posterior distribution (Fig. 3). The maximum carrying capacity was estimated to be 51,642 individuals per 20 km^2 (129.4 individuals per km^2), with approximately 0.46% of each grid cell's occupants were estimated to emigrate every generation (i.e., 2388 individuals at maximum carrying capacity). The ancestral effective population size was comparatively low and estimated at 100 individuals. All estimated parameters were significantly associated with the summary statistics components (all $p < 0.001$): however, the power of our parameter estimates was still relatively low (see R^2 and p in Table 2).

Final demographic and genetic models—The simulated genetic landscape under present-day conditions predicts widespread high genetic diversity throughout the Sierra Nevada Mountains and the north-central Great Basin (ca. 7–9 alleles per locality, on average). Further east, genetic diversity is dramatically reduced, and many localities are estimated to have, on average, a single locus of each simulated microsatellite. In the Mojave Desert, to the south, and the Great Salt Desert, to the east, respectively, the species is absent.

Under future climatic scenarios, genetic diversity is predicted to decline dramatically across the central Great Basin, with the exception of the areas surrounding the Columbia Plateau, the Ruby Mountains, and parts of the Colorado Plateau in southeastern Utah. The 2080p scenario predicts continued loss of allelic diversity in the Ruby and the northern Sierra Nevada Mountains, whereas genetic diversity is maintained in other areas (Fig. 2E, F).

Widespread declines are predicted in the number of individuals under the two future scenarios, with a 98% reduction being estimated—from ca. 1.92×10^7 individuals in the current simulation to, on average, 4.02×10^5 individuals in the 2080/2080p scenarios. Yet, the total allelic diversity loss is less drastic, with an allelic diversity loss of 15–20%. Average total allelic diversity of the current, 2080 and 2080p landscapes are, respectively, 71.35 ± 1.51 (standard deviation), 60.94 ± 1.14, and 56.94 ± 1.31. Although these models predict only moderate loss of genetic diversity at the species level, genetic diversity of individual demes is expected to experience greater declines. Individual populations are predicted to decline to 62–80% of their current average allelic diversity. Average allelic diversity of occupied cells is, respectively, 7.15 ± 0.02, 5.75 ± 0.06, and 4.41 ± 0.04 for the current, 2080, and 2080p simulations, indicating substantial reduction in genetic diversity.

DISCUSSION

We implement a novel method for predicting spatially explicit genetic and demographic landscapes of future populations using *Penstemon deustus* as a study system. This flexible framework uses carefully parameterized SDMs as estimates of the spatial distribution of suitable habitats and landscape dispersal permeability. Importantly, we use approximate Bayesian computation (ABC) to estimate key unknown demographic parameters based on population genetic data from empirical populations. Our approach accounts for system-specific climatic, geographic and biological complexity to estimate the neutral genetic diversity of populations. To our knowledge, this is the first method to provide future spatially explicit genetic estimates based on realistic climatic, demographic and genetic data.

Using demographic and genetically based models provides key advantages for quantifying the effects of future climate change relative to the use of SDMs alone. Habitat suitability values output from SDMs often do not reflect easily quantifiable characteristics of natural populations and, thus, are difficult to interpret in terms of the precise biological consequences of temporal or spatial changes. For instance, large reductions in areas of high habitat suitability values may result in less drastic local effects to populations in the future if overall habitat suitability remains above a certain threshold. Our simulations of *P. deustus* in the Sierra Nevada Mountains show that the amount of estimated changes under current vs. future conditions varies considerably depending on the inference method used (SDM-only in Fig. 2G; demographic and genetic estimates in Fig. 2H, I). Large differences between present-day and future habitat suitability are predicted when comparing SDM outputs alone. However, these differences do not appear to equally, or significantly, impact the distribution of genetic diversity when we employ demographic parameters, estimated from genetic data, into

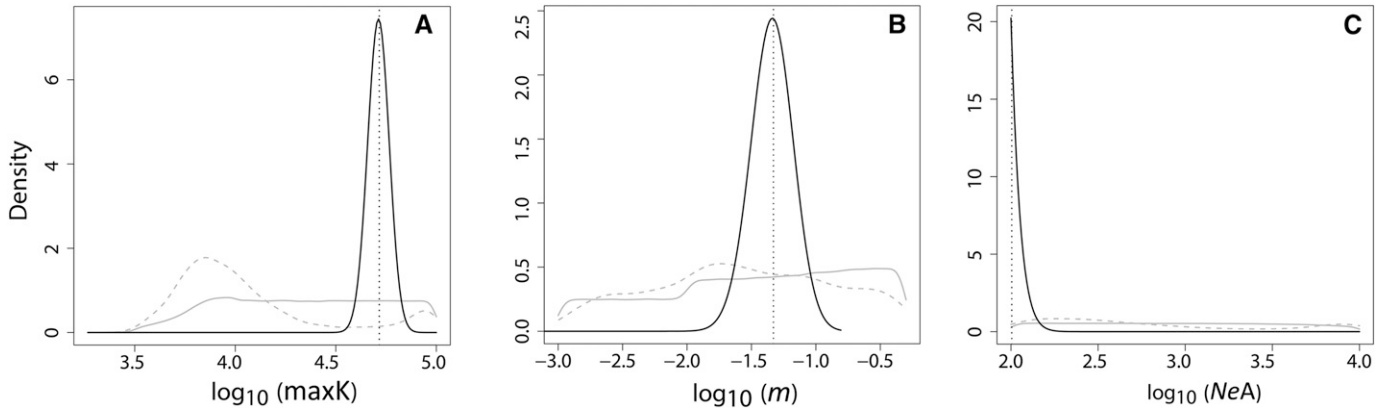

FIGURE 3 Distributions of the posterior probabilities of each estimated demographic parameter: long-term migration rate (m), maximum landscape carrying capacity (maxK, in terms of population), and an ancestral effective population size (N_{eA}). The posterior mode (dotted vertical black line), posterior (solid black line) and prior (solid gray line) distributions, and postsampling regression adjustment (dashed gray line) are shown. All values are in $\log_{10}$. Note that all parameters are estimated at the spatial resolution of simulations.

the predictions themselves. Conversely, subtle environmental changes in regions where local populations are near the very extremes of their ecological tolerances (i.e., localities usually characterized by low SDM suitability values) can have dramatic consequences. In our case study, a large portion of the central Great Basin transitions from possessing high population densities under present-day conditions to local extinction in future models (Fig. 2A–G).

Expected shifts in the geographic distribution of genetic diversity were also estimated here. Allelic diversity landscapes for both 2080 and 2080p remain constant throughout most of the species' predicted distribution, suggesting a balance between loss of diversity due to genetic drift with potential genetic gains due to migration and de novo mutations. However, in some regions (e.g., near Ruby and northern Sierra Nevada Mountains), genetic diversity is predicted to dramatically decrease under the 2080p scenario, suggesting a stronger local influence of genetic drift (carrying capacity of the landscape is fixed between these two time periods; Fig. 2E, F). Compared to the SDMs, these demographic and genetic-based models provide quantifiable estimates of demographic and genetic parameters (e.g., the number of individuals predicted at each cell, average allelic diversity) that present a more complete picture of the possible consequences of climate change.

Our parameter estimates were consistent with empirical data available for *P. deustus*. For instance, our estimate of maximum carrying capacity (maxK= 129.4 individuals per km^2) nicely matches recent census data (100–500 total individuals, as per Kramer et al., 2011). Further, the low number of migrations into adjacent demes (0.46% of each grid cell's occupants) is consistent with observed genetic and natural history data: *P. deustus* is primarily bee-pollinated, which likely increases population structure and genetic isolation relative to co-distributed congeners that are either avian- or wind-pollinated (Kramer et al., 2011). Despite these consistencies and our significant parameter estimates (all $p < 0.001$), the power of our parameter estimation was still low (R^2 and p in Table 2).

A critical step forward in this framework will be to evaluate model uncertainty and its effects on genetic estimates (Collevatti et al., 2015). It will be important to incorporate uncertainty introduced by future climate models and scenarios, as well as uncertainty resulting from the demographic parameter estimates, SDMs, and the conversion of SDMs into carrying capacity landscapes. At the moment, our models provide a new framework for realistic forecasts of genetic landscapes. These results, however, should be interpreted with caution until there is an improvement in how model uncertainty is directly incorporated into estimates and projections.

An important assumption of the framework implemented here is that local populations will keep tracking climatic changes as they have done in the past, or, in other words, that the demographic parameters estimated from empirical neutral genetic data will be appropriate to model biological responses into the future. This framework implies that lineages will continue to track climates, as opposed to adapt to new local environmental conditions—a statement not free of caveats (Rubidge et al., 2012). Mounting evidence has shown that populations can exhibit adaptive genetic changes over short evolutionary time periods (reviewed by Franks et al., 2014). One alternative to account for this possibility is to experimentally quantify genetic changes in response to temporal shifts in the environment, as has been done in studies that compare ancestral and descendant lineages raised in common gardens ("resurrection approach", Franks et al., 2008). Moreover, seed banks specifically designed to study evolution in ancestral and descendant lineages using the resurrection approach (Project Baseline; Franks et al., 2008; Etterson et al., 2016 in this special issue) now enable empirical quantification of spatiotemporal responses to strong environmental selection. We suggest that genetic data acquired from such efforts could be used to further assess the precision and relevance of the simulated spatiotemporally explicit neutral genetic landscapes that we present here. Comparing statistical differences between simulated genetic neutral data and observed spatiotemporal genetic changes will further improve measurements of selection strength and shed light on correlations between ecological drivers and genetic diversity.

Evolutionary seed databases, such as Project Baseline (Franks et al., 2008), a seedbank for understanding plant population responses to climate change, provide important opportunities to ground-truth future genetic estimates. This resource facilitates studies aimed at understanding evolutionary patterns and processes across space and time and can provide critical insight into the accuracy of future model projections. Another key area of future study should focus the effects local adaptation to environments through time (vs. climatic niche stability and spatial tracking, as assumed here). Modeling testing with ABC in conjunction with changes in species distribution model specificity (e.g., using different regularization multipliers in Maxent), different demographic transformations, and models built with specific lineages, provide a framework to study the effects of changes in ecological tolerances. The level of spatiotemporal niche stability could increase or decrease the spatial segregation of populations and genetic diversity. Lastly, simulations of selection across changing landscapes will help contrast potential signatures selection (vs. neutral landscapes as simulated here) and the effects of spatiotemporal changes in habitat.

Under the framework presented here, conservation strategies will be able to focus on lineages or populations that are particularly vulnerable in terms of demographic parameters and genetic diversity. Conservation strategies may be critically evaluated or adapted to the existing reserve network to potentially maximize genetic diversity or species abundance in a dynamic landscape. Applications of this method can also go beyond estimating the effects of climate change to incorporate other anthropogenic changes, including land use and the impacts of urbanization and deforestation.

With improved statistical pipelines and increasingly available genomic, population, and climate data, scientists will be able to provide more precise estimates of the genetic consequences of future climate change. Using available data on *P. duestus*, we successfully demonstrate this framework has the potential to be used on a wide range of taxa and scenarios. Our method can provide key insights into the spatiotemporal effects of current, past, and future distribution shifts—an approach that can inform how demographic shifts have shaped, and will continue to shape, biotas. Accordingly, we can potentially identify the specific circumstances and lineages where conservation is needed, leading to more efficient conservation practices.

ACKNOWLEDGEMENTS

We are grateful to Jeremy Van Derwall, Robert P. Anderson, and the Carnaval and Hickerson Laboratories. Funding was provided by a co-funded FAPESP (BIOTA, 2013/50297-0), National Science Foundation (DOB 1343578), and NASA Dimensions of Biodiversity

grant to A.C.C. and M.J.H., Project Baseline NSF grant (DEB-1142784) to S.J.F., and National Science Foundation award (DEB-1253710) to M.J.H.

AUTHOR CONTRIBUTIONS

J.L.B., J.J.W., and D.A.-S. each contributed equally to this research. J.J.W. developed and provided expertise on the study system. J.L.B. and D.A.S. performed analyses and developed the statistical framework. J.J.W., J.L.B., D.A.S., and A.C.C. wrote the paper, and S.J.F., M.J.H. provided insightful suggestions and comments during the design, analyses, and writing.

LITERATURE CITED

Alsos, I. G., T. Alm, S. Normand, and C. Brochmann. 2009. Past and future range shifts and loss of diversity in dwarf willow (*Salix herbacea* L.) inferred from genetics, fossils and modelling. *Global Ecology and Biogeography* 18: 223–239.

Alsos, I. G., D. Ehrich, W. Thuiller, P. B. Eidesen, A. Tribsch, P. Schönswetter, C. Lagaye, et al. 2012. Genetic consequences of climate change for northern plants. *Proceedings. Biological Sciences* 279: 2042–2051.

Alvarado-Serrano, D. F., and L. L. Knowles. 2014. Ecological niche models in phylogeographic studies: Applications, advances and precautions. *Molecular Ecology Resources* 14: 233–248.

Anderson, R. P. 2013. A framework for using niche models to estimate impacts of climate change on species distributions. *Annals of the New York Academy of Sciences* 1297: 8–28.

Anderson, R. P., and A. Raza. 2010. The effect of the extent of the study region on GIS models of species geographic distributions and estimates of niche evolution: Preliminary tests with montane rodents (genus *Nephelomys*) in Venezuela. *Journal of Biogeography* 37: 1378–1393.

Assis, J., E. Serrão, B. Claro, C. Perrin, and G. A. Pearson. 2014. Climate-driven range shifts explain the distribution of extant gene pools and predict future loss of unique lineages in a marine brown alga. *Molecular Ecology* 23: 2797–2810.

Barbet-Massin, M., F. Jiguet, C. H. Albert, and W. Thuiller. 2012. Selecting pseudo-absences for species distribution models: How, where and how many? *Methods in Ecology and Evolution* 3: 327–338.

Barrett, R. D., and D. Schluter. 2008. Adaptation from standing genetic variation. *Trends in Ecology & Evolution* 23: 38–44.

Beaumont, M. A., R. Nielson, C. Robert, J. Hey, O. Gaggiotti, L. L. Knowles, A. Estoup, et al. 2010. In defense of model-based inference in phylogeography. *Molecular Ecology* 19: 436–446.

Beaumont, M. A., W. Zhang, and D. Balding. 2002. Approximate Bayesian computation in population genetics. *Genetics* 162: 2025–2035.

Bertorelle, G., A. Benazzo, and S. Mona. 2010. ABC as a flexible framework to estimate demography over space and time: Some cons, many pros. *Molecular Ecology* 19: 2609–2625.

Blum, M. G. B. 2010. Approximate Bayesian computation: A nonparametric perspective. *Journal of the American Statistical Association* 105: 1178–1187.

Boria, R. A., L. E. Olson, S. M. Goodman, and R. P. Anderson. 2014. Spatial filtering to reduce sampling bias can improve the performance of ecological niche models. *Ecological Modelling* 275: 73–77.

Boulesteix, A. L., and K. Strimmer. 2007. Partial least squares: A versatile tool for the analysis of high-dimensional genomic data. *Briefings in Bioinformatics* 8: 32–44.

Brown, J. L. 2014. SDMtoolbox: A python-based GIS toolkit for landscape genetic, biogeographic and species distribution model analyses. *Methods in Ecology and Evolution* 5: 694–700.

Brown, J. L., and L. L. Knowles. 2012. Spatially explicit models of dynamic histories: examination of the genetic consequences of Pleistocene glaciation and recent climate change on the American Pika. *Molecular Ecology* 21: 3757–3775.

Chan, L., J. L. Brown, and A. D. Yoder. 2011. Integrating statistical genetic and geospatial methods brings new power to phylogeography. *Molecular Phylogenetics and Evolution* 59: 523–537.

Collevatti, R. G., L. C. Terribile, J. A. F. Diniz-Filho, and M. S. Lima-Ribeiro. 2015. Multi-model inference in comparative phylogeography: An integrative approach based on multiple lines of evidence. *Frontiers in Genetics* 6: 31.

Csilléry, K., M. G. B. Blum, O. E. Gaggiotti, and O. Francois. 2010. Approximate Bayesian computation (ABC) in practice. *Trends in Ecology & Evolution* 25: 410–418.

Currat, M., N. Ray, and L. Excoffier. 2004. SPLATCHE: A program to simulate genetic diversity taking into account environmental heterogeneity. *Molecular Ecology Notes* 4: 139–142.

Dawson, T. P., S. T. Jackson, J. I. House, I. C. Prentice, and G. M. Mace. 2011. Beyond predictions: Biodiversity conservation in a changing climate. *Science* 332: 53–58.

Dellicour, S., S. Fearnley, A. Lombal, S. Heidl, E. Dahlhoff, N. Rank, and P. Mardulyn. 2014. Inferring the past and present connectivity across the range of a North American leaf beetle: Combining ecological-niche modeling and a geographically explicit model of coalescence. *Evolution* 68: 2371–2385.

Espíndola, A., L. Pellissier, L. Maiorano, W. Hordijk, A. Guisan, and N. Alvarez. 2012. Predicting present and future intra-specific genetic structure through niche hindcasting across 24 millennia. *Ecology Letters* 15: 649–657.

Etterson, J. R., S. J. Franks, S. J. Mazer, R. G. Shaw, N. L. Soper Gorden, H. E. Schneider, J. J. Weber, et al. 2016. Project Baseline: An unprecedented resource to study plant evolution across space and time. *American Journal of Botany* 103: 164–173.

Excoffier, L., and H. E. L. Lischer. 2010. Arlequin suite ver 3.5: A new series of programs to perform population genetics analyses under Linux and Windows. *Molecular Ecology Resources* 10: 564–567.

Excoffier, L., J. Novembre, and S. Schneider. 2000. SIMCOAL: A general coalescent program for the simulation of molecular data in interconnected populations with arbitrary demography. *Journal of Heredity* 91: 506–509.

Fitzpatrick, M. C., and S. R. Keller. 2015. Ecological genomics meets community-level modelling of biodiversity: Mapping the genomic landscape of current and future environmental adaptation. *Ecology Letters* 18: 1–16.

Fordham, D. A., B. W. Brook, C. Moritz, and D. Nogués-Bravo. 2014. Better forecasts of range dynamics using genetic data. *Trends in Ecology & Evolution* 29: 436–443.

Frankham, R., K. Lees, M. E. Montgomery, P. R. England, E. H. Lowe, and D. A. Briscoe. 1999. Do population size bottlenecks reduce evolutionary potential? *Animal Conservation* 2: 255–260.

Franks, S. J., J. C. Avise, W. E. Bradshaw, J. K. Conner, J. R. Etterson, S. J. Mazer, R. G. Shaw, and A. E. Weis. 2008. The resurrection initiative: Storing ancestral genotypes to capture evolution in action. *BioScience* 58: 870–873.

Franks, S. J., J. J. Weber, and S. N. Aitken. 2014. Evolutionary and plastic responses to climate change in terrestrial plant populations. *Evolutionary Applications* 7: 123–139.

Fuchs, J., J. L. Parra, S. M. Goodman, M. J. Raherilalao, J. Vanderwal, and R. C. Bowie. 2013. Extending ecological niche models to the past 120 000 years corroborates the lack of strong phylogeographic structure in the crested drongo (*Dicrurus forficatus forficatus*) on Madagascar. *Biological Journal of the Linnean Society* 108: 658–676.

Fuller, R. N., and R. del Moral. 2003. The role of refugia and dispersal in primary succession on Mount St. Helens, Washington. *Journal of Vegetation Science* 14: 637–644.

Garner, A., J. L. Rachlow, and J. F. Hicks. 2005. Patterns of genetic diversity and its loss in mammalian populations. *Conservation Biology* 19: 1215–1221.

Gehara, M. C., K. Summers, and J. L. Brown. 2013. Population expansion, isolation and selection: Novel insights on the evolution of color diversity in the strawberry poison frog. *Evolutionary Ecology* 27: 797–824.

Graham, C. H., J. VanDerWal, S. J. Phillips, C. Moritz, and S. E. Williams. 2010. Dynamic refugia and species persistence: Tracking spatial shifts in habitat through time. *Ecography* 33: 1062–1069.

He, Q., D. L. Edwards, and L. L. Knowles. 2013. Integrative testing of how environments from the past to the present shape genetic structure across landscapes. *Evolution* 67: 3386–3402.

Hijmans, R. J., S. E. Cameron, J. L. Parra, P. G. Jones, and A. Jarvis. 2005. Very high resolution interpolated climate surfaces for global land areas. *International Journal of Climatology* 25: 1965–1978.

Humphries, C. J., P. H. Williams, and R. I. Vane-Wright. 1995. Measuring biodiversity value for conservation. *Annual Review of Ecology and Systematics* 26: 93–111.

IPCC. 2014. Climate Change 2014: Mitigation of Climate Change. Contribution of Working Group III to the Fifth Assessment Report of the Intergovernmental Panel on Climate Change. Cambridge University Press, Cambridge, UK.

Jump, A. S., R. Marchant, and J. Peñuelas. 2009. Environmental change and the option value of genetic diversity. *Trends in Plant Science* 14: 51–58.

Kartesz, J. T. 1999. A synonymized checklist of the vascular flora of the U.S., Canada, and Greenland. *In* J. T. Kartesz and C. A. Meacham [eds.], Synthesis of the North American flora, version 1.0. North Carolina Botanical Garden, Chapel Hill, North Carolina, USA.

Kartesz, J. T. 2015. The Biota of North America Program (BONAP). North American Plant Atlas, available at http://bonap.net/napa. Chapel Hill, North Carolina, USA [maps generated from Kartesz, J.T. 2015. Floristic synthesis of North America, version 1.0. Biota of North America Program (BONAP), in press].

Kimura, M., and W. H. Weiss. 1964. The stepping stone model of genetic structure and the decrease of genetic correlation with distance. *Genetics* 49: 561–576.

Knowles, L. L., and D. F. Alvarado-Serrano. 2010. Exploring the population genetic consequences of the colonization process with spatio-temporally explicit models: Insights from coupled ecological, demographic and genetic models in montane grasshoppers. *Molecular Ecology* 19: 3727–3745.

Kramer, A. T. 2008. Ecological genetics of *Penstemon* in the Great Basin, USA. Ph.D. dissertation, University of Illinois at Chicago, Chicago, Illinois, USA.

Kramer, A. T., J. Fant, and M. V. Ashley. 2011. Influences of landscape and pollinators on population genetic structure: Examples from three *Penstemon* (Plantaginaceae) species in the Great Basin. *American Journal of Botany* 98: 109–121.

Leinonen, T., R. B. O'Hara, J. Cano, and J. Merilä. 2008. Comparative studies of quantitative trait and neutral marker divergence: a meta-analysis. *Journal of Evolutionary Biology* 21: 1–17.

Leuenberger, C., and D. Wegmann. 2010. Bayesian computation and model selection without likelihoods. *Genetics* 184: 243–252.

Marriage, T. N., S. Hudman, M. E. Mort, M. E. Orive, R. G. Shaw, and J. J. Kelly. 2009. Direct estimation of the mutation rate at dinucleotide microsatellite loci in *Arabidopsis thaliana* (Brassicaceae). *Heredity* 103: 310–317.

Marske, K. A., R. A. B. Leschen, and T. R. Buckley. 2012. Concerted versus independent evolution and the search for multiple refugia: Comparative phylogeography of four forest beetles. *Evolution* 66: 1862–1877.

Merilä, J., and P. Crnokrak. 2001. Comparison of genetic differentiation at marker loci and quantitative traits. *Journal of Evolutionary Biology* 14: 892–903.

Merow, C., M. J. Smith, and J. A. Silander. 2013. A practical guide to MaxEnt for modeling species' distributions: What it does, and why inputs and settings matter. *Ecography* 36: 1058–1069.

Neuenschwander, S., C. R. Largiader, N. Ray, M. Currat, P. Vonlanthen, and L. Excoffier. 2008. Colonization history of the Swiss Rhine basin by the bullhead (*Cottus gobio*): Inference under a Bayesian spatially explicit framework. *Molecular Ecology* 17: 757–772.

Parmesan, C., and G. Yohe. 2003. A globally coherent fingerprint of climate change impacts across natural systems. *Nature* 421: 37–42.

Peterson, A. T., J. Soberón, R. G. Pearson, R. P. Anderson, E. Martínez-Meyer, M. Nakamura, and M. B. Araújo. 2011. Ecological niches and geographic distributions. Princeton University Press, Princeton, New Jersey, USA.

Phillips, S. J., R. P. Anderson, and R. E. Schapire. 2006. Maximum entropy modeling of species geographic distributions. *Ecological Modelling* 190: 231–259.

Phillips, S. J. , and M. Dudík 2008. Modeling of species distributions with Maxent: New extensions and a comprehensive evaluation. *Ecography* 31: 161–175.

Prentis, P. J., J. R. Wilson, E. E. Dormontt, D. M. Richardson, and A. J. Lowe. 2008. Adaptive evolution in invasive species. *Trends in Plant Science* 13: 288–294.

Radosavljevic, A., and R. P. Anderson. 2014. Making better Maxent models of species distributions: Complexity, overfitting, and evaluation. *Journal of Biogeography* 41: 629–643.

Rangel, T. F., J. A. F. Diniz-Filho, and L. M. Bini. 2010. SAM: A comprehensive application for Spatial Analysis in Macroecology. *Ecography* 33: 46–50.

Ray, N., M. Currat, M. Foll, and L. Excoffier. 2010. SPLATCHE2: A spatially explicit simulation framework for complex demography, genetic admixture and recombination. *Bioinformatics* 26: 2993–2994.

Reed, D. H., and R. Frankham. 2001. How closely correlated are molecular and quantitative measures of genetic variation? A meta-analysis. *Evolution* 55: 1095–1103.

Rizzon, C., L. Ponger, and B. S. Gaut. 2006. Striking similarities in the genomic distribution of tandemly arrayed genes in *Arabidopsis* and rice. *PLoS Computational Biology* 2: e115.

Rubidge, E. M., J. L. Patton, M. Lim, A. C. Burton, J. S. Brashares, and C. Moritz. 2012. Climate-induced range contraction drives genetic erosion in an alpine mammal. *Nature Climate Change* 2: 285–288.

Shcheglovitova, M., and R. P. Anderson. 2013. Estimating optimal complexity for ecological niche models: A jackknife approach for species with small sample sizes. *Ecological Modelling* 269: 9–17.

Singarayer, J. S., and P. J. Valdes. 2010. High-latitude climate sensitivity to ice-sheet forcing over the last 120 kyr. *Quaternary Science Reviews* 29: 43–55.

Takahashi, M., and I. Katano. 2010. Genetic diversity increases regional variation in phenological dates in response to climate change. *Global Change Biology* 16: 373–379.

Taubmann, J., K. Theissinger, K. A. Feldheim, I. Laube, W. Graf, P. Haase, J. Johannesen, and S. U. Pauls. 2011. Modelling range shifts and assessing genetic diversity distribution of the montane aquatic mayfly *Ameletus inopinatus* in Europe under climate change scenarios. *Conservation Genetics* 12: 503–515.

Tavaré, S., D. J. Balding, R. C. Griffiths, and P. Donnelly. 1997. Inferring coalescence times from DNA sequence data. *Genetics* 145: 505–518.

van der Linden, P., and J. F. B. Mitchell. 2009. ENSEMBLES: Climate Change and its Impacts: Summary of research and results from the ENSEMBLES project. Met Office Hadley Centre, Exeter, UK.

Wegmann, D., C. Leuenberger, and L. Excoffier. 2009. Efficient approximate Bayesian computation coupled with Markov chain Monte Carlo without likelihood. *Genetics* 182: 1207–1218.

Wegmann, D., C. Leuenberger, S. Neuenschwander, and L. Excoffier. 2010. ABCtoolbox: A versatile toolkit for approximate Bayesian computations. *BMC Bioinformatics* 11: 116.

Wold, H. 1966. Estimation of principal components and related methods by iterative least squares. *In* P. R. Krishnaiah [ed.], Multivariate analysis, 391–420. Academic Press, New York, New York, USA.

Yannic, G., L. Pellissier, J. Ortego, N. Lecomte, S. Couturier, C. Cuyler, C. Dussault, and S. D. Côté. 2014. Genetic diversity in caribou linked to past and future climate change. *Nature Climate Change* 4: 132–137.